

DOI: 10.2478/rgg-2025-0018

Received: 18 July 2025 / Accepted: 14 November 2025

Published online: 2 December 2025





ORIGINAL ARTICLE

Effects of observation loss in geodetic determination of horizontal displacements

Joanna Swatowska 10 1* and Przemysław Kuras 10 1

¹Faculty of Geo-Data Science, Geodesy, and Environmental Engineering, AGH University of Krakow, A. Mickiewicza 30, 30-059 Krakow, Poland

Abstract

Regular monitoring of dams is fundamental to ensuring their safety, stability, and smooth operation. However, during the measurement phase, a number of obstacles are encountered that are often difficult to predict at the planning stage of the observation campaign. In such situations, the surveyor must decide whether to continue all planned observations, which may involve a significant extension of working time. An alternative is to reduce the number of observations deliberately, provided the required accuracy and reliability of the data are ensured. This paper examines the impact of missing observations on the position errors of control network points. Using an angular-linear network as an example, a simulation was carried out by excluding observation stations selected at random from subsequent adjustments and by checking its effect on the final result. Additionally, the possibility of removing from the adjustment those observations that were considered problematic for measurement due to various types of obstacles was verified. The results of the conducted studies show that the cautious station elimination prevents network weakening. The necessary removal of problematic observations can be implemented already at the measurement stage. These findings highlight the significant trend of decreasing accuracy in determining the positions of network points. After eliminating 15% of the observations, the control network maintained high accuracy, with the resulting RMSE changing by no more than 10%.

Key words: geodetic monitoring, horizontal displacements, control network, water dams, loss of observations

Introduction

1.1 Importance of dam monitoring

Monitoring of dams is crucial to ensuring their safety, stability and smooth operation (Milanović et al., 2019). As Szostak-Chrzanowski and Massiéra (2006) point out, monitoring should be an integral part of the entire dam life cycle. Regular analysis of monitoring data helps to adapt structures to changing operational and natural conditions and increases the safety of hydraulic structures.

Throughout the world, dam monitoring is recognised as an essential part of the safety management of hydro-technical facilities. Organisations of experts such as the International Commission on Large Dams (ICOLD) and the US Army Corps of Engineers (USACE) emphasise the need for continuous oversight of dams at every stage of their operation - from the construction process through to operation and subsequent upgrades and maintenance. International Commission on Large Dams (ICOLD) recommends implementing monitoring systems to detect irregularities early and prevent their consequences. Dam monitoring components include routine visual inspections, specialised inspections, parameter and equipment monitoring, automation, monitoring system upgrades and much more. In line with current regulations (US Army Corps of Engineers, 2018), the USACE operates a comprehensive risk-based dam safety programme in accordance with the Federal Guidelines for Dam Safety. Its main objective is to ensure that all dams and their components are designed, built, operated and maintained as safely as possible, minimising the risk of failure and ensuring their stability throughout their lifetime.

The maintenance of dams is regulated by national legislation, which sets out the rules for their operation, technical inspection and supervision. These regulations are intended to ensure the safety of

^{*}jswat@agh.edu.pl

hydraulic structures (Gruszecka, 2016; Dmitruk, 2022). In Poland, geodetic control and inventory surveys of hydraulic structures are compulsory under current legislation (Act, 1994, 2017; Regulation, 2007). Polish law (Act, 1994) requires regular inspections at least once a year to assess the technical condition of a building. In addition, the technical performance and service value of the entire structure should be assessed at least once every five years.

The lack of systematic monitoring of the technical condition of hydraulic structures can pose several dangers and hazards, ranging from damage to the dam itself and economic losses to soil erosion and water pollution, and even threatening the lives of people living below the structure. Failures pose a serious threat to people, infrastructure and the environment. One of the most drastic examples of the consequences of inadequate measurement in recent years is the Oroville Dam disaster in California. The dam was severely damaged, prompting the evacuation of more than 180,000 people from neighbouring valley areas (Hollins et al., 2018). In February 2017, the dam faced a major crisis due to a sharp rise in the reservoir's water level following heavy rainfall. It turned out that displacement and erosion monitoring were not carried out frequently enough, limiting the ability to respond quickly to changes in dam condition (Bea and Johnson, 2017).

In addition to measuring the dam's displacement, it is important to monitor its surroundings. Threats to dam stability can come not only from the structure itself but also from external factors such as geological conditions, climate, and human activities. The Vajont dam disaster in Italy demonstrates the importance of monitoring the dam environment. A landslide of rock debris into the reservoir created a giant wave which overflew the dam, causing massive damage and the death of many people (Fiedler, 2007).

Regular monitoring and data analysis enable hydraulic structures to be adapted to changing operational and natural conditions, improving safety and providing information for theoretical models (Nowak et al., 2022). The information obtained from monitoring is also used to assess how dams respond to changes in reservoir water levels and to seasonal environmental factors such as temperature fluctuations or other climatic variables (Oro et al., 2016; Tretyak and Palianytsia, 2022).

1.2 Methods for monitoring horizontal displacements

"Monitoring of hydrotechnical structures – especially damming structures - refers to systematic observations, measurements and studies of these structures for the assessment of their technical condition and safety" (Kledyński, 2011a). The development of control and measurement methods and equipment enables the use of various systems to control dams (Kledyński, 2011b). Chrzanowski et al. (2011) discuss considerations for selecting dam deformation monitoring techniques, focusing primarily on reliability and efficiency. They point out several technologies and their advantages and disadvantages.

One of the most accurate devices used for monitoring is the pendulum. However, according to Barzaghi et al. (2018), this method can be used only at predefined points within the dam structure. In addition, the pendulum data are collected inside the dam structure and cannot correctly account for crest displacements. In many papers, deformations obtained from the pendulum sensor are compared with those from other measurement techniques. Barzaghi et al. (2018) compare the results obtained with this method to the GNSS technique, acknowledging that the pendulum is a more accurate method for determining dam displacements. Ribeiro et al. (2008) reached the same conclusions.

Standard measurement methods include the static method based on Global Navigation Satellite Systems (GNSS). It has been widely used worldwide for several decades (Ehiorobo and Irughe-Ehigiator, 2011; Taşçi, 2008). It is an effective method for assessing dam deformation and structural integrity, allowing high precision

and automation (Scaioni et al., 2018). Studies have shown that GNSS techniques can achieve millimetre-level accuracy in monitoring dam displacements (Cardoso et al., 2020; Maltese et al., 2021). In addition, they do not require visibility between measured points, as the accuracy of position determination depends on the visibility of satellites in the satellite constellation, the reflection of satellite signals, and refraction phenomena in the ionosphere and troposphere (Agapie Mereuta et al., 2022). Maltese et al. (2021) highlighted the capability for comprehensive monitoring of dam displacements using satellite geodetic techniques, including GNSS and PS-InSAR.

Another dam monitoring method gaining popularity is terrestrial laser scanning (Alba et al., 2006; Zaczek-Peplinska et al., 2013; Šarkanović Bugarinović et al., 2023). This technology offers advantages such as fast data acquisition, high point density and comprehensive geometric information (Zaczek-Peplinska et al., 2013). Using terrestrial laser scanning, Negrila and Onose (2013) obtained accuracies of a few to a dozen millimetres. More recent methods also include Interferometric Synthetic Aperture Radar (InSAR) from satellites (Mazzanti et al., 2021) and from the ground (Talich, 2016). InSAR can enhance dam safety by providing high-resolution measurements of cyclic settlement (Aswathi et al., 2022). This technology is characterised by very high temporal and spatial resolution, high accuracy, and a wide field of view (Dwitya et al., 2024; Rebmeister et al., 2025). Talich (2016) reports that some points in the upper parts of the Concrete Hydropower Dam Orlík show movements of approximately 0.9 mm.

Total station measurement of angular-linear networks is the most standard surveying method and offers the highest absolute accuracy. It is used on various sites, including landslides and bridges, but especially on hydraulic structures. Total stations can detect small displacements with high accuracy, making them suitable for landslide monitoring (Amaral et al., 2020) and bridge utility assessments (Merkle and Myers, 2004). In addition, Kuras et al. (2018) describe the application of total station geodetic monitoring to observe the displacement of an earth-filled dyke subjected to varying loads. Furthermore, automated monitoring systems use electronic total stations to enable continuous, interval-based observations of hydraulic structures such as dams (Staroverov and Haikin, 2020).

1.3 Optimisation of geodetic observations for the purposes of determining displacements

The typical processing of angular-linear network measurement data involves using the least-squares method to adjust the network and assess the measurement accuracy. The standard deviation of the position of control points for the typical dam, e.g. the Jamishan dam, reported by Farzaneh et al. (2021), did not exceed 1.30 mm. In contrast, Bagherbandi (2016) achieved 0.2 mm and 0.1 mm in the x and y directions, respectively, when analysing a simulated geodetic network located at the Kungsbäck laboratory at the main campus of the University of Gävle. Such accuracies are achievable under controlled and stable conditions. We achieved slightly lower accuracies, because the analysed network was exposed to variable terrain and weather conditions.

Data redundancy should be used to achieve better adjustment results. Increasing the number of observations benefits the accuracy and reliability of the network (Prószyński, 2014). However, this is often made difficult by the rising cost of performing the work. In addition, over time, more and more survey points become inaccessible due to changing site conditions, such as vegetation overgrowth, the appearance of trees or dense thickets (Salagean et al., 2017). There are cases when observing restrictions during geodetic network surveying are unavoidable. Nowak and Odziemczyk (2018) noted that moderate redundancy was sufficient and selected redundant observations for reduction in a strict manner. They used a covariance matrix for their analyses.

Sometimes the weather conditions are unfavourable, limiting



Figure 1. Location of the water dam in Niedzica (shown in red; CRS: PL-2000, EPSG:2178) (source: www.geoportal.gov.pl)

the number of measurement sites on a given day and requiring an extra 24 hours for measurement. It is advisable to speed up the measurement as much as possible without sacrificing accuracy. Therefore, in our article, a simulation was carried out to exclude individual observations or sites from subsequent adjustments and to assess the effect on the final result. The research task is to determine the minimum number of observations required to achieve the required measurement accuracy.

In addition, unexpected obstructions may arise during the survey, such as overgrown intervisibility lines or trees, parked vehicles, or larger construction equipment. The question then arises: how relevant are such lines of sight for carrying out the adjustment? Our paper will examine whether the maximum possible number of observations should be pursued and to what extent inaccessible points are necessary to achieve the required accuracy.

2 Czorsztyn-Niedzica dam

One of the key elements of hydrotechnical infrastructure in Poland is the Czorsztyn-Niedzica dam (Figure 1). The dam, located at 173+300 kilometres of the Dunajec River, created Lake Czorsztyn, which has a total capacity of 231.9 million m³ (Dziewański, 1998). There are numerous active landslides around this reservoir.

The area to the north of the dam lies on the Carpathian flysch bedrock, which consists mainly of alternating layers of sandstone, shale, and siltstone. The geological formation of the Pieniny Rock Belt predominates in the southern and eastern parts. It is characterised by a variety of sedimentary rocks, including limestone and marl (Golonka et al., 2018).

The Czorsztyn-Niedzica dam is an example of an earth dam sealed with a clay core located in the central part of the body. The maximum height from the gallery walkway is 56 m, and the structure itself extends 404 m east-west. The crown of the dam measures 7 m in width and is entirely open to pedestrians and authorised vehicles (company ZEW Niedzica S.A.).

3 Surveying network structure

The need for continuous monitoring of the technical condition of hydraulic structures involves systematic measurements of horizontal and vertical displacements (Novak et al., 2007). The horizontal displacement monitoring system includes an angular-linear network that covers both the dam site and adjacent areas (Odziemczyk, 2014; Scaioni et al., 2018). An important condition for these networks is the need to maintain intervisibility lines between the sites (Lu et al., 2014).

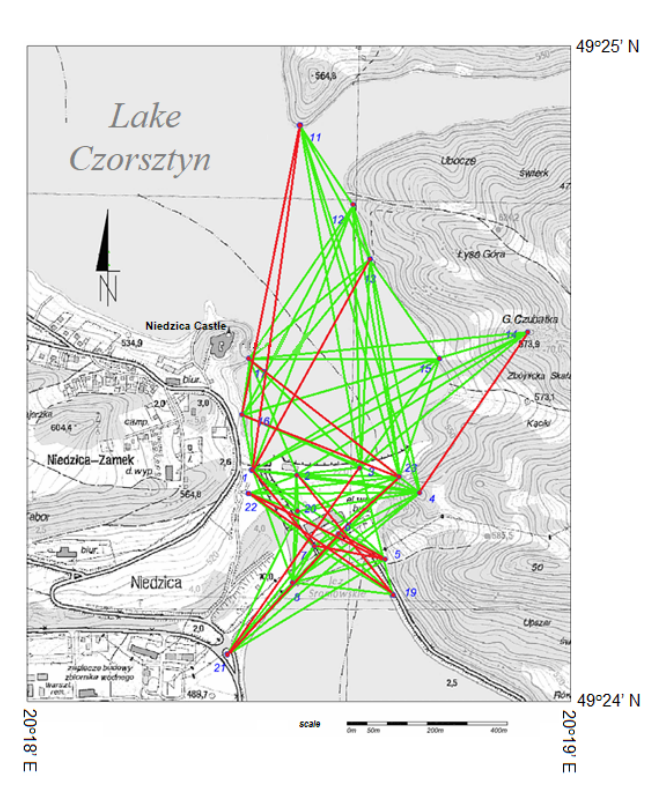


Figure 2. Measured (green) and unavailable (red) lines-of-sight in the angular-linear network

Measurement points are located on the crest of the dam, on structural elements of the dam that are accessible for measurement from the ground surface and on the banks of the lakes that are in the immediate vicinity of the facility. The network comprises 20 points. They have been stabilised using pillars planted either below ground frost depth or directly in the rock, without a pillar (2 points). All survey poles have been equipped with metal plates with bushings, fitted for the forced centring of tribrachs, which have screws specially adjusted for this purpose ending in spherical heads (Guler et al., 2006; Ortelecan et al., 2012). Figure 2 shows the distribution of angular-linear network points, measured lines of sight (green), and lines of sight lost over the years (red).

Despite the meticulously selected locations for the individual points in the survey network, not all points meet the aforementioned condition of visibility between each other. This is due to the intensive development of infrastructure around the dam and the ongoing expansion of tree cover (including in the National Park adjacent to the dam). In addition, points 11 and 14 have proven unsuitable for measurement due to their specific locations, difficult accessibility, and insufficient space around them for measurement.

Monitoring of the technical condition of the Niedzica dam and its adjacent areas is conducted annually. Angular and linear measurements are taken to determine the dam's displacement. For this type of measurement, a point position error of 1 mm after adjustment is required

A robotic total station, the Leica Nova MS50, was used for the measurements, which are characterized by a standard deviation of $\pm 3^{\text{CC}}$ for angle measurements and $\pm (1 \text{ mm} + 1.5 \text{ ppm})$ for distance measurements. All observations were performed using prisms; therefore, given the size of the network, the limitation of the distance measurement range to 1000 m did not pose a problem. Automatic targeting technology was used to smoothly execute the five series until the standard deviation of the mean direction was less than 2^{CC} . Atmospheric parameters were also measured each time to reduce distance (Zaczek-Peplinska et al., 2018).

In the survey execution diagram (Figure 3), points numbered 11 and 14 were not used as measurement sites, and all questionable

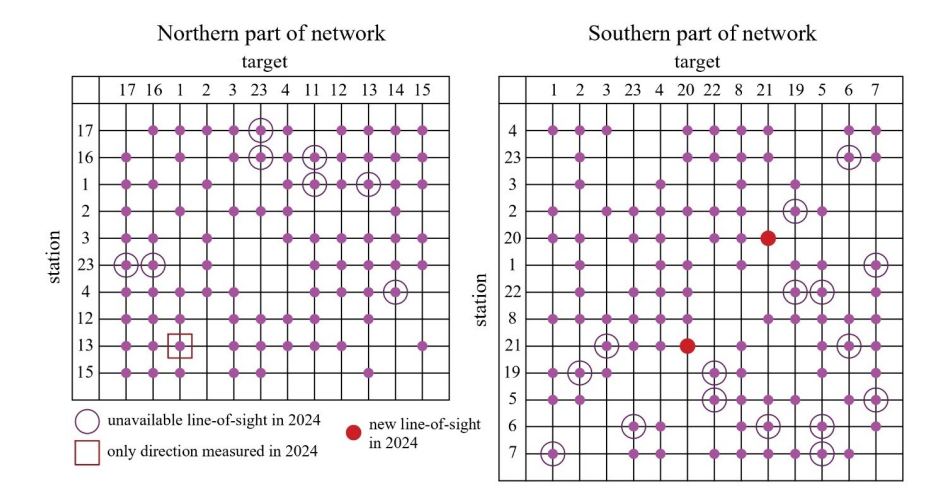


Figure 3. Diagram of measured sites divided into northern and southern parts of the network

intervisibility lines from 2022 were not used due to unavailability. The diagram, which dates back a few years, shows how the number of lines of sight is decreasing (Salagean et al., 2017). The observed lines of sight are shown in Figure 3. A total of 151 directional observations and 81 length observations were measured.

4 Network adjustment

The process of adjusting the measurement network was carried out in stages. Observational data were divided into two groups: directional and length observations. The two data sets were adjusted in separate adjustment modules to determine the correct standard deviations of the individual observations. In addition, outlier observations were rejected. The large number of redundant observations enabled the standard deviations to be determined with high reliability (Bergkvist, 2015). The appropriately weighted observations were then used for the final combined adjustment after combining the two data types. The adjustments were performed without deforming the network, using the minimum number of elements to eliminate the defect (Grafarend and Sansò, 1985).

The adjustment process began with angular observations, including 151 directions. For the calculations, à priori errors of σ_K = 1^{cc} were assumed. A total of 18 outlier observations (12% of all), for which the correction exceeded 4^{cc}, were discarded. The average directional correction was 1.7^{cc}. The standard deviation σ_0 of the adjusted directions was 2.22^{cc}. This value was taken as the mean direction error for the final adjustment of the directions.

This was followed by an adjustment of 81 linear observations. À priori errors of σ_d = 1 mm + 1 ppm were assumed. Subsequent iterations resulted in the rejection of a total of five outlier observations (6% of all) for which the correction exceeded 1.2 mm. The average absolute value of distance correction was 0.36 mm. The standard deviation σ_0 of the adjusted distances was 0.37. This value was taken as the mean distance error for the final distance adjustment. The unit error values for direction and distance are the same year on year, with a tolerance of a few per cent. The aim of performing separate adjustments for directions and distances was to reject some outlier observations and estimate the errors of the individual observations.

In total, across all adjustment stages, 28 values were discarded out of 232 observations of directions and distances, representing 12% of the total. The standard deviation σ_0 of the final adjustment, taking into account directions and lengths, was 0.99, indicating a correct balance of the angular and linear observations. The largest corrections were: for direction –5 $^{\rm CC}$ and for length, 0.87 mm. In

Table 1. Angular-linear network information and adjustment statistics

Output adjustment				
Number of points	21			
Directions	129			
Lengths	75			
Total number of observations	204			
Redundant observations	147			
σ_0	0.99			
RMSE [mm]	0.78			
$\sigma_{\rm XY_11}$ [mm]	1.13			
$\sigma_{XY_{-}14}$ [mm]	1.12			

addition, the position errors of the control network points after adjustment do not exceed 1.20 mm. The points with the most unfavourable geometric positions have the largest position errors, i.e., 11 (σ_{XY} = 1.13 mm) and 14 (σ_{XY} = 1.12 mm). The position errors of the other points do not exceed 0.75 mm. Later in this paper, the position errors of the points from this adjustment will be the starting values for further analyses and will be denoted as σ_{XY} init.

Table 1 provides basic information about the angular-linear network subjected to output adjustment, together with its statistics. Symbols used in the table: σ_0 – standard deviation, RMSE – root mean square error of point position, σ_{XY_i} – the situational position error of the i-th point. The formulas used to calculate the specified parameters are presented below:

$$\sigma_0 = \sqrt{\frac{p_i v_i^2}{n - u}} \tag{1}$$

where p_i – the weight of observation, v_i – the residual of observation, n – the number of observations, u – the number of unknowns;

$$\sigma_{XY_i} = \sqrt{\sigma_{X_i}^2 + \sigma_{Y_i}^2} \tag{2}$$

where σ_{Xi} , σ_{Yi} – the standard deviation of the X and Y coordinates of the *i*-th point;

$$RMSE = \sqrt{\frac{1}{m} \sum_{i=1}^{m} \sigma_{XY_i}^2}$$
 (3)

where m – the number of points.

Table 2 lists the number of rejected outlier observations from

Table 2. Number of rejected outlier observations from individual adjustments

Adjustment	Rejected outlier observations	Share of rejected observations from a given adjustment	
directions	18 directions	12%	
distances	5 distances	6%	
overall	4 directions and 1 distance	2%	
TOTAL	28	12%	

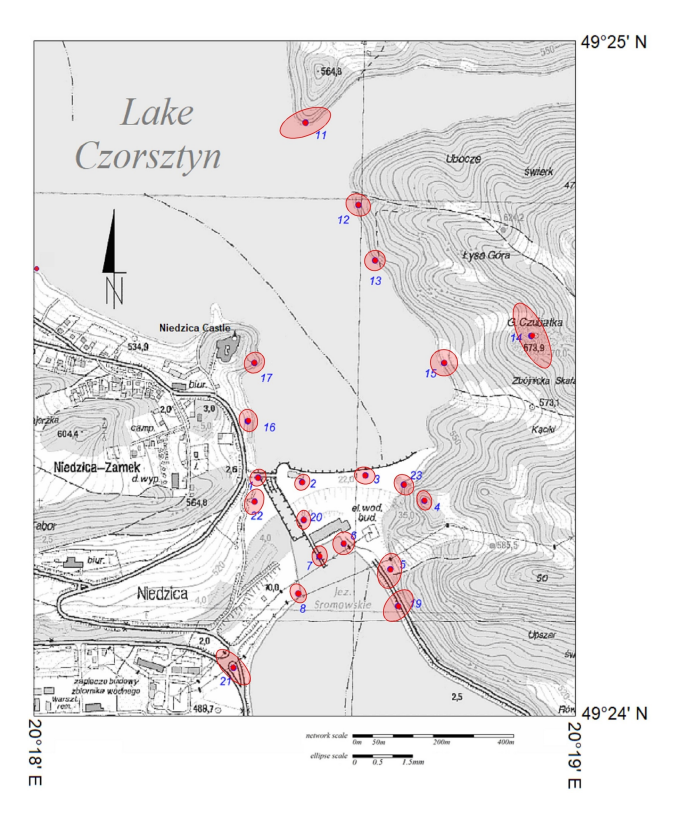


Figure 4. Error ellipses for control network points

each adjustment, and their percentages in relation to all observations used in the calculation module. Figure 4 shows the error ellipses of the control network points.

5 Observation reduction procedures and analyses

5.1 Elimination of sites

Due to unfavourable conditions, i.e. difficult field conditions, unfavourable weather, a lack of time to make the necessary number of observations, specific survey sites may need to be bypassed in order to speed up the survey as much as possible. Although such elimination carries some risk of reducing measurement accuracy and/or lowering the network's reliability, in many situations it is necessary to maintain surveying continuity.

Four simulations are shown below, each involving the exclusion of individual sites from successive stepwise adjustments. Each of the four paths involves eliminating three sites and has been prepared completely independently of the others. Points to be removed from the calculation process were selected at random. This involved drawing one site for elimination at a time, making an adjustment without observations from that site, then drawing further sites for

Table 3. Eliminated sites from individual simulations

	Path 1	Path 2	Path 3	Path 4
Drawing 1	20	21	22	13
Drawing 2	8	3	23	7
Drawing 3	17	15	13	16

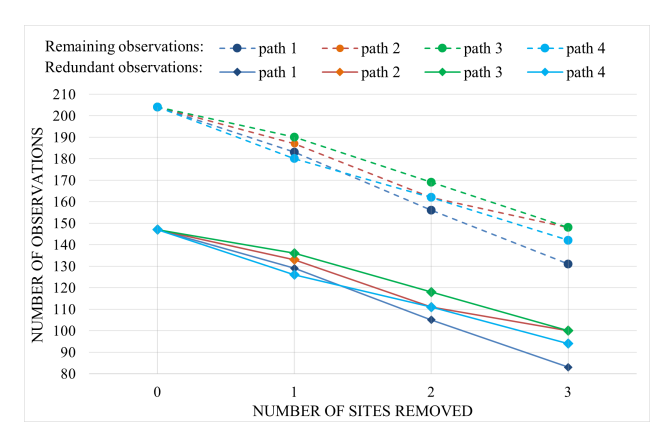


Figure 5. Number of remaining and redundant observations from the four paths of random site elimination

elimination and repeating the calculation process. Finally, a number of analyses were performed to assess the impact of these operations on the final outcome. For this purpose, the obtained standard deviations σ_0 , the RMSE of point position, and the position errors of points 11 and 14, which have the most unfavourable geometric positions in the angular–linear network, were collated. The sites that were eliminated at random from each pathway are shown in Table 3. In addition, the number of remaining (dashed line) and redundant (solid line) observations across the four paths of random site elimination can be seen in the graph (Figure 5).

In the first step of the elimination process, site 20 was selected and removed from the control and measurement network. All angular and linear observations associated with this point were discarded. The entire angular-linear network was readjusted. The largest corrections for angular and linear observations were 5 $^{\rm CC}$ and 1.13 mm, respectively. A slight increase in the standard deviation σ_0 was observed. The RMSE of point position increased by 0.03 mm relative to that from the reference adjustment, and the position errors of points numbered 11 and 14 increased by 0.01 mm.

In the next step, site 8 was selected, and removed from the network. The computational process was repeated with fewer redundant observations, and several accuracy analyses were performed. The largest corrections for angular and linear observations were identified, equal to $5^{\rm cc}$ and 1.06 mm, respectively. In addition, a further increase in the standard deviation $\sigma_{\rm O_i}$ accompanied by a simultaneous increase in the RMSE and the position errors of the analysed points, was observed.

The last site selected for elimination was point number 17. The horizontal network was readjusted. The largest correction for angular observations was 5^{CC}, and for length, -1.11 mm. The standard deviation increased slightly, while the RMSE and point position errors unexpectedly increased by 0.12 mm and an average of 0.23 mm, respectively, compared to those from previous calculations.

Subsequent computational paths were conducted similarly. Observations from the selected sites were removed; the remaining observations were adjusted, and the results were collated. The analysed parameters, i.e., standard deviation σ_0 , RMSE, and position errors for points 11 and 14 from all adjustments, are shown in Table 4. Additionally, the table includes a single network evaluation criterion; the network's internal reliability f. The reliability of a geodetic network depends primarily on the number of observations,

Table 4. Horizontal network adjustment statistics for site elimination

	Path 1		Path 2			
Number of eliminated point	20	8	17	21	3	15
f	0.70	0.67	0.63	0.71	0.68	0.67
σ_0	0.99	1.00	1.04	1.00	0.99	1.02
RMSE [mm]	0.81	0.88	0.99	0.79	0.86	0.99
σ_{XY_11} [mm]	1.14	1.17	1.32	1.14	1.20	1.25
$\sigma_{XY_{-14}}$ [mm]	1.13	1.15	1.45	1.13	1.42	1.48
		Path 3			Path 4	
Number of eliminated point	22	23	13	13	7	16
f	0.71	0.69	0.67	0.70	0.68	0.66
σ_0	0.98	0.98	0.99	1.01	1.00	0.96
RMSE [mm]	0.78	0.83	0.95	0.90	0.92	0.96
$\sigma_{XY_{-11}}$ [mm]	1.12	1.17	1.40	1.36	1.35	1.38
$\sigma_{XY_{-14}}$ [mm]	1.11	1.12	1.15	1.16	1.15	1.21

particularly redundant ones (Prószyński, 2014). This parameter was computed using the formula:

$$f = 1 - \frac{u}{n} \tag{4}$$

5.2 Analysis of the results obtained

Standard deviation σ_0

In Figure 6 shows that for path 1, the standard deviation increases successively. In contrast, σ_0 shows no clear trend across the other paths. When outlier observations are removed, the value of σ_0 is obviously reduced. However, in the site elimination procedure described in this paper, points for removal were selected at random. As a result, the changing value of σ_0 will be influenced by the weights of the observations. This irregular volatility is as expected. To avoid it, each time a site is removed, the adjustment would have to be done in three stages, i.e. separately for directions and distances – to determine their respective standard deviations – and then together. However, as all σ_0 obtained are within the range calculated for a confidence level of 1– α = 95%, it is not necessary to count them in this way. Therefore, there are no grounds to reject the adjustment results.

The confidence interval for the standard deviation in the general population (σ) can be calculated by trying to estimate the standard deviation s. The confidence interval for 1- α = 95% can be calculated from the statistical test (Burdick and A., 1992), defined by the formula:

$$\left(\sqrt{\frac{(n-1)s^2}{\chi^2_{\alpha/2}}}, \sqrt{\frac{(n-1)s^2}{\chi^2_{1-\alpha/2}}}\right) = (0.89; 1.12)$$
 (5)

where: s=0.99- standard deviation calculated from the sample, n=147- sample size, $\chi^2_{\alpha/2}=182.459-$ point of the same chi-square distribution with exactly $\alpha/2$ of the area under the curve to the right of $\chi^2_{\alpha/2}$, $\chi^2_{1-\alpha/2}=115.326-$ point of the chi-square distribution with n-1 degrees of freedom at which exactly $\alpha/2$ of the area under the curve is to the left of $\chi^2_{1-\alpha/2}$.

RMSE of point position

In Figure 7, the RMSE of the point position is shown to change across the four paths of elimination of individual sites from the adjustment. In all cases, the aforementioned parameter increases with each iteration. Furthermore, it has been observed that for path numbers 1, 2, and 3, this process starts with a small jump, followed

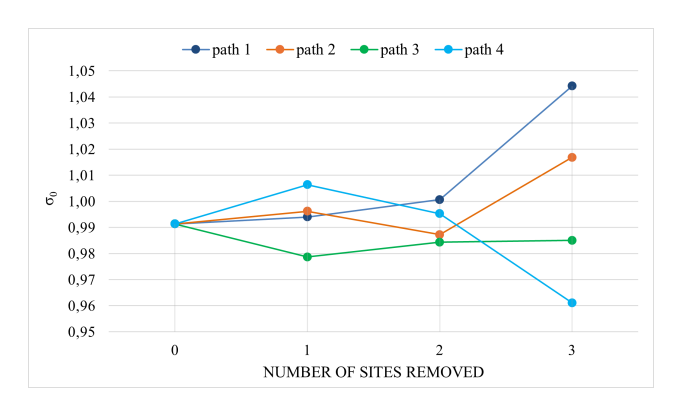


Figure 6. Standard deviation σ_0 of the four elimination paths of the individual sites

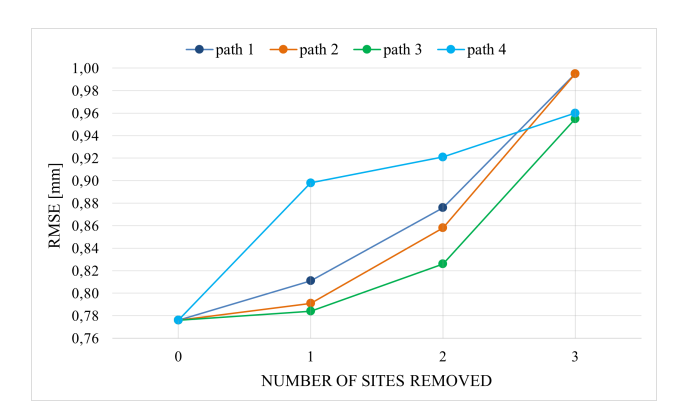


Figure 7. RMSE of point position from four elimination paths for the individual sites

by a sharp increase in subsequent iterations. This may indicate that the points selected in the second and third draws play a key role in adjusting the control and measurement network in Niedzica. In contrast, those from the first elimination are less important in the aforementioned calculation process. In contrast, the situation is radically different for path 4. The analysed parameter remains in an upward trend, but in a different pattern: a sharp spike at the beginning followed by a slow increase thereafter.

When excluding subsequent sites, the key question is what RMSE error limit the network is expected to meet. Often, it is determined by the facility manger's requirements or by regulations. It is influenced by various factors. Nevertheless, the measurement should be performed in optimal weather conditions, and the intervisibility lines should be cleared. When all of the above is taken into account, it can be concluded that the direction and length measurements should yield the lowest root-mean-square error in point position, often within 1-2 mm for typical dams (Farzaneh et al., 2021). In the angular-linear network in question, this error did not exceed 1 mm, indicating a well-designed network and proper points distribution.

Maximum point position error $\sigma_{\mbox{\scriptsize max}}$

Two points, numbered 11 (σ_{XY_11} = 1.13 mm) and 14 (σ_{XY_14} = 1.12 mm) were analysed, which have the most unfavourable geometric positions in the angular-linear network. The former is the northernmost point of the network, while the latter is the easternmost.

Figure 8 shows the position error of the first point. Within $\sigma_{XY_11},$ magnitudes of the order of 1.1–1.5 mm appear. For path 1, the values slowly increase, with a sharp spike at the end. In contrast, there is a slight decrease in the position error at point 11 in path 3, but it then increases further down the path and ends with a similar spike. The final sharp increases may be due to the elimination of points from the northern part of the grid (numbers 17 and

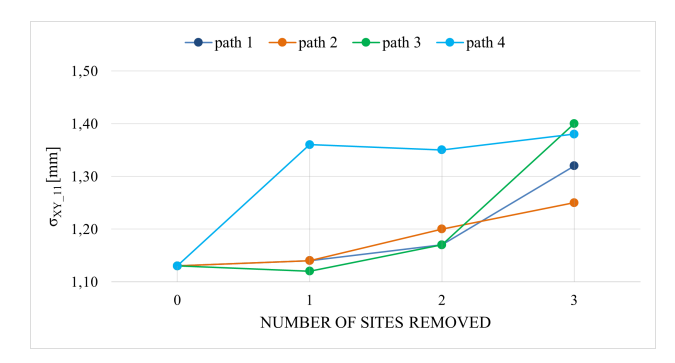


Figure 8. Position error of point 11 from the 4 elimination paths of the individual

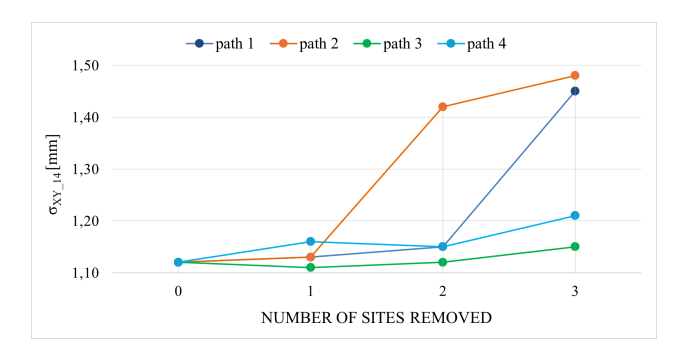


Figure 9. Error in the position of point 14 of the four elimination paths of the individual sites

13), which has weakened the network geometry in that area.

The error for path 2 shows a similar trend, steadily increasing. Although the finally removed point 15 is also located in the northern part of the angular-linear network, no sharp spike was observed at the end, as with the values from paths 1 and 3. In the case of path 4, there is an abrupt spike at the beginning, followed by a period of stabilization and even a slight decline, ending with a slight increase.

Figure 9 shows the position errors for point 14 along the four paths. Despite the two pints analysed being in similar locations, few parallels were found in the graphs. The main similarity between the graphs for σ_{XY_11} and σ_{XY_14} is the range of values, which is 1.1 to 1.5 mm.

An apparent similarity was observed for path 1. At the beginning, a slight increase is visible, which turns into a sharp spike in the final phase.

For path 2, an initial slight increase in σ_{XY_14} is observed, followed by a sharp increase that is clearly greater than that for σ_{XY_11} . Finally, in both cases, the error values continue to increase, but to a much lesser extent.

The position error of point 14 within path 3 does not show a clear upward trend, as it initially decreases and then returns to its initial value. Although the upward trend in the further course is similar for both charts, the spike sizes differ. In the first graph, there is a sharp spike at the end, while in the second, it is much smaller.

For the last path in question, an increase in σ_{XY_12} , is observed at the beginning, which later gives way to a decrease. In the final phase, however, the values rise again, restoring the original trend. A similar pattern, albeit with a noticeably larger first spike, is also present in the previous graph.

In general, there is an intuitive trend of worsening position error for points 11 and 14 as the number of observations decreases. However, there are slight deviations from this relationship that arise from a coincidence between the covariance matrix of unknowns and σ_0 .

Table 5. Lines of sight eliminated from individual adjustments

Adjustment number	Eliminated lines-of-sight From (to) To (from)		Problem with the lines-of-sight
1	13	12	bushes, poor visibility
1	13	15	busiles, poor visibility
	1	12	
2	1	13	railing
	1	15	
	1	16	lines-of-sight
3	1	17	over water, lateral
	16	17	refraction phenomenon
	23	7	crane
4	23	20	trees
	23	22	tiees
5	7	4	avana
	7	23	crane
6	22	7	forest, clearing

5.3 Elimination of observations

In 1997, when the angular-linear network for monitoring the displacement of the Niedzica dam's grid points was established, changes in the surroundings of the established points and the emergence of terrain obstacles were difficult to predict. Growth of scrub, growing trees, and developing infrastructure can hinder access to specific sites, such as measurement sites, reduce visibility in the field, slow measurements, and sometimes even make them impossible. Occasionally, such obstacles are not detected and removed before the survey, which means that personnel responsible for fieldwork have to extend their working hours. Sometimes, despite efforts, some obstacles prove impossible to remove, or there is not enough time to do so. Examples include situations where it would be necessary to clear a forest, dismantle temporary buildings or road barriers. In such cases, the simplest solution is to omit observations between the sites concerned. In order to avoid this type of situation and speed up the work, a network analysis can be carried out in advance to determine whether all lines of sight are necessary for the adjustment and whether some can be omitted during the measurement. It is important here not to lose the required accuracy.

Following a detailed field interview, seven trouble spots in the angular-linear network under study were identified. The problems encountered during the measurement are analysed below. Table 5 lists all identified problematic lines of sight. Six groups are distinguished, comprising 1 to 3 sight lines, with indicated issues between points.

The first distinguished group includes lines of sight with poor visibility, caused by overgrown thickets along the eastern shore of Lake Czorsztyn, located below the dam. The second cluster includes sight lines, for which the barrier in front of pillar 1 is an obstacle, making accurate targeting difficult. The third set has the most lines of sight eliminated. They are arranged along the western shore, which is particularly heavily exposed to sunlight before noon. Water and terrain heat up at different rates, resulting in lateral refraction. The fourth group is associated with point 23, which is overgrown with numerous trees. On the eastern shore of the lake is the Pieniny National Park. An additional obstacle is a crane which cannot always be moved for technical reasons. The problem with the next set is also a crane. The last group includes observations between points 22 and 7. In this case, a forest is the obstacle.

Once the problematic connections were identified, adjustments were made and removed from the individual calculation processes. Six separate adjustments were made because it was not clear which

Table 6. Statistics of the individual adjustments after removal of observations

Adjustment number	Point number	σ _{XY_init} [mm]	σ _{XY} [mm]
	12	0.74	0.79
1	13	0.61	0.66
	15	0.60	0.69
	12	0.74	0.78
2	13	0.61	0.63
	15	0.60	0.61
2	16	0.38	0.63
3	17	0.44	0.59
	7	0.39	0.39
,	20	0.33	0.33
4	22	0.43	0.44
	23	0.42	0.49
	4	0.23	0.23
5	7	0.39	0.42
	23	0.42	0.44
-	7	0.39	0.41
6	22	0.43	0.46

lines of sight were problematic at any given time or in what configuration. Table 6 shows the position error values of σ_{XY} points from the adjustments for which observations from the specific groups were removed, together with the values from the output adjustment $\sigma_{XY_init}.$ For the five groups, the differences in the collated errors are of the order of hundredths of a millimetre. However, slightly larger differences were noted for group 3, equal to 0.25 mm for point 16 and 0.15 mm for point 17. From a practical point of view, the changes observed are insignificant.

On the other hand, the number of angular and linear observations remaining after the removal of problematic connections, together with the results obtained and the analyses performed, is summarised in 0. Accordingly, the obtained standard deviation σ_0 , the RMSEs of point positions and the position errors of points 11 and 14 were collected. At the top of the table are the results of the reference adjustment, denoted as 0. In addition, a collective adjustment was performed at the very end, taking into account all the removed sight lines. Point 7 of the table below show the results obtained. After discarding the problematic observations, 109 directions and 64 lengths remained, representing 84% and 85% of the observations from the reference adjustment, respectively.

5.4 Analysis of the results obtained

Standard deviation σ_0

Table 7 includes the values of σ_0 obtained from the adjustments for individual groups (1–6), from the reference (0) and collective (7) adjustment. Removing a small number of observations during the elimination process had no significant effect on the obtained values of σ_0 , as evidenced by the absence of meaningful changes in these values in cases 1–6 relative to adjustment no. 0. In the collective adjustment (7), after eliminating all problematic observations from the dataset, the resulting standard deviation was 0.91.

In addition, all standard deviations obtained were within the range calculated for a confidence level of $1-\alpha=95\%$, providing no grounds for rejection of the adjustment results. The confidence interval for $1-\alpha=95\%$ was calculated using formula (5), and the values obtained were (0.89; 1.12).

Table 7. Statistics of individual adjustments after removal of observa-

Adjustment number	Number of observations after removal: directions lengths	σ_{0}	RMSE [mm]	σ _{XY_11} [mm]	[©] XY_14 [mm]
0	129 75	0.99	0.78	1.13	1.12
1	126 73	1.00	0.80	1.16	1.13
2	126 74	0.98	0.79	1.16	1.11
3	123 72	0.94	0.80	1.20	1.11
4	124 72	0.98	0.77	1.12	1.11
5	126 73	0.98	0.77	1.12	1.11
6	128 74	0.99	0.78	1.13	1.12
7	109 64	0.91	0.86	1.35	1.11

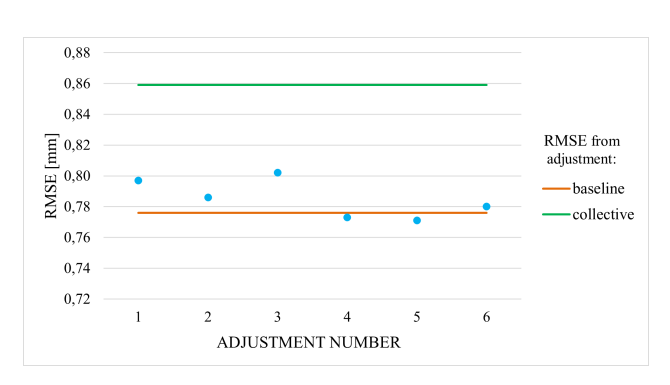


Figure 10. RMSE of point position from adjustments of observations without elimination relative to RMSE from the reference and collective adjustments

RMSE of point position

Figure 10 shows how RMSE changes for each group relative to the value of this error determined for the reference (0.78 mm) and collective adjustment (0.86 mm). The RMSE values for adjustments 0–6, listed in Table 7, do not differ significantly from one another. This is due to the small changes in the number of observations removed in the individual adjustments. For the collective adjustment, after removing a total of 31 observations, the parameter increased by 0.08 mm relative to adjustment no. 0 (approx. 10%).

Maximum point position error σ_{max}

As with the analysis of site elimination results, two points, 11 and 14, which have the most unfavourable geometric positions in the network, were analysed.

Figure 11 and Table 7 show the σ_{XY_11} values obtained from the adjustments of the six groups, as well as the reference and collective adjustments. Most of the adjustments yielded larger σ_{XY_11} values than those of the reference adjustment. The highest value of σ_{XY_11} from the adjustments 1–6, equal to 1.20 mm, was found for adjustment 3. After performing the collective adjustment and eliminating all problematic connections, σ_{XY_11} was found to equal 1.35 mm.

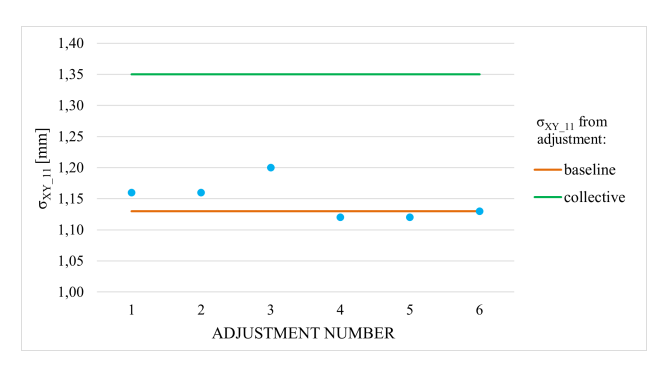


Figure 11. Position error of point 11 from adjustments of observations without problematic ones relative to σ_{XY_11} from the reference and collective adjustments

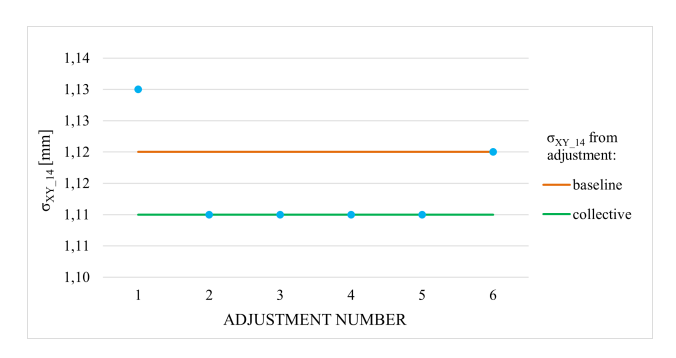


Figure 12. Position error of point 14 from the adjustments of nonproblematic observations relative to σ_{XY} 14 from the reference and collective adjustments

The increment between the collective adjustment value and the reference is 0.22 mm (approx. 19%).

Figure 12 and Table 7 show the position error of the second point in question. Although both the analysed point and most of the removed observations are located in the northern part of the network, the variation in σ_{XY_14} values is insignificant.

The effect was expected, and the aim was to see how the error would increase observations were eliminated.

Conclusions

The main objective of this paper was to determine whether it is necessary to obtain as many observations as possible during fieldwork and whether measurements from hard-to-reach points are necessary to achieve the required accuracy.

When removing outlier observations, the value of σ_0 is obviously diminished. However, the site-elimination procedure described in this paper selected the points to be removed at random. As a result, the changing value of σ_0 will be influenced by the remaining observations' weights in the adjustment and by the factual errors of the observation values.

In all situations, the root-mean-square error of point position increased with each iteration of input data elimination. However, this error did not exceed the 1 mm limit in any of the paths. This indicates an excellent network design. The largest RMSE value was $% \left(1\right) =\left(1\right) +\left(1\right) +$ 0.99 mm, and the largest σ_{XY_11} and $\sigma_{XY_14} values$ were 1.40 mm and 1.48 mm.

The research indicates that careful analysis of point elimination allows a better assessment of the impact of missing data on the adjustment process. Thoughtful site selection prevents network weakening and preserves access to displacement and deformation information in the study area.

Another objective of this study was to verify whether it is possible to remove problematic individual observations from the adjustment. Elimination of all observations considered to be outliers resulted in the lowest standard deviation of all analysed variants in the collective adjustment, at 0.91.

To summarise, the elimination of problematic observations can be effectively carried out already at the measurement stage. Even after removing the 31 observations (15% of all) classified as outliers, the control network maintained high accuracy, with the resulting RMSE increasing by only 0.08 mm relative to the reference adjust-

Funding

Financial support of AGH University of Krakow - subsidy no. 16.16.150.545

References

Act (1994). Act of 7 July, 1994 Construction Law. Act. Journal of Laws 2025, Item 725, Poland.

Act (2017). Act of of 20 July, 2017 Water Law. Act. Journal of Laws 2025, Item 216, Poland.

Agapie Mereuta, I., Luca, M., Gherasim, P. M., and Dominte Croitoru, V. (2022). Design Of GNSS Networks For Monitoring Earth Dams Deformations. Journal of Applied Life Sciences and Environment, 54(4):354-369, doi:10.46909/journalalse-2021-

Alba, M., Fregonese, L., Prandi, F., Scaioni, M., Valgoi, P., et al. (2006). Structural monitoring of a large dam by terrestrial laser scanning. International Archives of Photogrammetry, Remote Sensing and Spatial Information Sciences, 36(5):6.

Amaral, P., Malheiro, A., Marques, F., Moniz, L., Furtado, S., and Loura, N. (2020). The Use of Total Station for Monitoring Mass Movements: Application to Fajazinha Landslide at Flores Island (Azores Archipelago), page 59-62. Springer International Publishing, doi:10.1007/978-3-030-34397-2_12.

Aswathi, J., Binoj Kumar, R., Oommen, T., Bouali, E., and Sajinkumar, K. (2022). InSAR as a tool for monitoring hydropower projects: A review. Energy Geoscience, 3(2):160-171, doi:10.1016/j.engeos.2021.12.007.

Bagherbandi, M. (2016). Deformation monitoring using different least squares adjustment methods: A simulated study. KSCE Journal of Civil Engineering, 20(2):855-862, doi:10.1007/s12205-015-0454-5.

Barzaghi, R., Cazzaniga, N., De Gaetani, C., Pinto, L., and Tornatore, V. (2018). Estimating and Comparing Dam Deformation Using Classical and GNSS Techniques. Sensors, 18(3):756, doi:10.3390/s18030756.

Bea, R. and Johnson, T. (2017). Root causes analyses of the Oroville dam gated spillway failures and other developments. Cal Alumni Association: Berkeley, CA, USA.

Bergkvist, J. (2015). Optimal Design of Network for Control of Total Station Instruments. Master's thesis, KTH, School of Architecture and the Built Environment (ABE), Urban Planning and Environment, Geodesy and Satellite Positioning.

Burdick, R. K. and A., G. F. (1992). Confidence Intervals on Variance Components.

Cardoso, F. H. C., Giorgini, M. G., and Paula, A. D. (2020). Diretrizes para o monitoramento de deformações e deslocamentos em barragens e estruturas de mineração utilizando GNSS. In Congresso Brasileiro de Mecânica dos Solos e Engenharia Geotécnica, Cobramseg, page 1415-1421. ABMS, doi:10.4322/cobramseg.2022.0178.

Chrzanowski, A., Szostak, A., and Steeves, R. (2011). Reliability and efficiency of dam deformation monitoring schemes. In Proceedings of the 2011 Annual Conference of Canadian Dam Association (CDA/ACB), Fredericton, NB, Canada, volume 15.

Dmitruk, Z. (2022). Zbiorniki zaporowe – aktualne zagadnienia

- ich funkcjonowania i oceny stanu bezpieczeństwa (Damming reservoirs - current issues concerning their operation and safety status assessment). GOSPODARKA WODNA, 1(10):4–12, doi:10.15199/22.2022.10.1.
- Dwitya, R., Hendrianto Pratomo, A., Agung Cahyadi, T., Rianto Budi Nugroho, A., Prio Utomo, D., and Sulo, C. (2024). Slope Stability Monitoring of Hydroelectric Dam and Upstream Watershed Areas Utilizing Satellite Interferometric Synthetic Aperture Radar (InSAR). IOP Conference Series: Earth and Environmental Science, 1339(1):012037, doi:10.1088/1755-1315/1339/1/012037.
- Dziewański, J. (1998). Warunki geologiczno-inżynierskie podłoża Zespołu Zbiorników Wodnych Czorsztyn-Niedzica i Sromowce Wyżne im. Gabriela Narutowicza na Dunajcu (Geological-engineering conditions of the substrate of water dams Czorsztyn and Sromowce Wyżne). Kraków: IGSMIE PAN Inst. Gosp. Sur. Min. Energ.
- Ehiorobo, J. O. and Irughe-Ehigiator, R. (2011). Monitoring for horizontal movement in an earth dam using differential GPS. Journal of Emerging Trends in Engineering and Applied Sciences,
- Farzaneh, S., Safari, A., and Parvazi, K. (2021). Improving Dam Deformation Analysis Using Least-Squares Variance Component Estimation and Tikhonov Regularization. Journal of Surveying Engineering, 147(1), doi:10.1061/(asce)su.1943-5428.0000339.
- Fiedler, K. (2007). Awarie i katastrofy zapór-zagrożenia, ich przyczyny i skutki oraz działania zapobiegawcze: praca zbiorowa (Dam failures and disasters - hazards, their causes and effects, and preventive measures). Instytut Meteorologii i Gospodarki Wodnej,
- Golonka, J., Krobicki, M., and Waśkowska, A. (2018). The Pieniny Klippen Belt in Poland. Geology, Geophysics and Environment, 44(1):111, doi:10.7494/geol.2018.44.1.111.
- Grafarend, E. W. and Sansò, F. (1985). Optimization and Design of Geodetic Networks. Springer Berlin Heidelberg, doi:10.1007/978-3-642-70659-2.
- Gruszecka, A. (2016). Wodne budowle piętrzące. Nadzór nad stanem technicznym i stanem bezpieczeństwa (Hydraulic Structures. Supervision of Technical Condition and Safety). Kontrola Państwowa, 61(5 (370):102-115.
- Guler, G., Kilic, H., Hosbas, G., and Ozaydin, K. (2006). Evaluation of the movements of the dam embankments by means of geodetic and geotechnical methods. Journal of surveying engineering, 132(1):31-39, doi:10.1061/(ASCE)0733-9453(2006)132:1(31).
- Hollins, L. X., Eisenberg, D. A., and Seager, T. P. (2018). Risk and Resilience at the Oroville Dam. Infrastructures, 3(4):49, doi:10.3390/infrastructures3040049.
- International Commission on Large Dams (ICOLD) (2018). Dam Surveillance Guide.
- Kledyński, Z. (2011a). Monitoring i diagnostyka budowli hydrotechnicznych. cz. 1 (Monitoring and diagnostics of hydrotechnical structures. P. 1). Nowoczesne Budownictwo Inżynieryjne, 35(2):54-61.
- Kledyński, Z. (2011b). Monitoring i diagnostyka budowli hydrotechnicznych. cz. 2 (Monitoring and diagnostics of hydrotechnical structures. P. 2). Nowoczesne Budownictwo Inżynieryjne, 36(3):36-38.
- Kuras, P., Ortyl, L., Owerko, T., and Borecka, A. (2018). Geodetic monitoring of earth-filled flood embankment subjected to variable loads. Reports on Geodesy and Geoinformatics, 106(1):9-18, doi:10.2478/rgg-2018-0009.
- Lu, Z., Qu, Y., and Qiao, S. (2014). Geodesy: Introduction to Geodetic Datum and Geodetic Systems. Springer Berlin Heidelberg, doi:10.1007/978-3-642-41245-5.
- Maltese, A., Pipitone, C., Dardanelli, G., Capodici, F., and Muller, J.-P. (2021). Toward a Comprehensive Dam Monitoring: On-Site and Remote-Retrieved Forcing Factors and Resulting Displacements (GNSS and PS-InSAR). Remote Sensing, 13(8):1543, doi:10.3390/rs13081543.
- Mazzanti, P., Antonielli, B., Sciortino, A., Scancella, S., and Bozzano,

- F. (2021). Tracking Deformation Processes at the Legnica Glogow Copper District (Poland) by Satellite InSAR—II: Żelazny Most Tailings Dam. Land, 10(6):654, doi:10.3390/land10060654.
- Merkle, W. J. and Myers, J. J. (2004). Use of the total station for load testing of retrofitted bridges with limited access. In Liu, S.-C., editor, Smart Structures and Materials 2004: Sensors and Smart Structures Technologies for Civil, Mechanical, and Aerospace Systems, volume 5391, page 687. SPIE, doi:10.1117/12.539992.
- Milanović, P., Maximovich, N. G., and Meshcheriakova, O. (2019). Monitoring, page 109-114. Springer International Publishing, doi:10.1007/978-3-030-18521-3_8.
- Negrila, A. and Onose, D. (2013). Dam monitoring using terrestrial laser scanning. Journal of Geodesy and Cadastre, (15):149-158.
- Novak, P., Moffat, A., Nalluri, C., and Narayanan, R. (2007). Hydraulic Structures (4th Edition). CRC Press.
- Nowak, B., Ptak, M., and Sojka, M. (2022). Monitoring of the Technical Condition and Optimisation of the Functioning of Small Hydraulic Structures in Poland: The Case Study of the Oświecim Weir. Buildings, 12(10):1527, doi:10.3390/buildings12101527.
- Nowak, E. and Odziemczyk, W. (2018). Impact analysis of observation coupling on reliability indices in a geodetic network. Reports on Geodesy and Geoinformatics, 106(1):1-7, doi:10.2478/rgg-2018-0008.
- Odziemczyk, W. (2014). Analiza stałości bazy odniesienia na przykładzie monitoringu przemieszczeń pionowych Zapory Zatonie (Analysis of reference points stability on the example of Zatonie Water Dam horizontal displacements monitoring). In Kulesza, J. and Wyczałek, I., editors, Teoretyczne Podstawy Budownictwa (Theoretical Foundations of Civil Engineering), pages 19-26. Publishing House of the Warsaw University of Technology.
- Oro, S., Mafioleti, T., Chaves Neto, A., Garcia, S., and Neumann Júnior, C. (2016). Study of the influence of temperature and water level of the reservoir about the displacement of a concrete dam. International Journal of Applied Mechanics and Engineering, 21(1):107-120, doi:10.1515/ijame-2016-0007.
- Ortelecan, M., Ciotlaus, A., Salagean, T., Ficior, D., Pop, N., Luput, I., and Vele, D. (2012). Considerations Regarding Hydro Power Station Monitoring Objectives Through Geodetic Measurements. Bulletin UASVM Horticulture, 69:2.
- Prószyński, W. (2014). Seeking realistic upper-bounds for internal reliability of systems with uncorrelated observations. Geodesy and Cartography, 63(1):111-121, doi:10.2478/geocart-2014-0009.
- Rebmeister, M., Schenk, A., Weisgerber, J., Westerhaus, M., Hinz, S., Andrian, F., and Vonié, M. (2025). Ground-based InSAR and GNSS integration for enhanced dam monitoring. Applied Geomatics, 17(2):393-400, doi:10.1007/s12518-025-00622-w.
- Regulation (2007). Regulation of the Minister of the Environment of April 20, 2007 on the technical conditions to be met by hydraulic engineering structures and their location. Act. Journal of Laws, 2007, No. 86, Item 579, Poland.
- Ribeiro, F., Fazan, J., Netto, N., Blitzkow, D., Da Fonseca Junior, E., Cintra, J., Fiorini, A., and Neves, C. (2008). Comparison between geodetic technology and plumb lines in monitoring of displacements on Itaipu Dam. In 13th International Symposium on Deformation Measurements and Analysis, International Federation of Surveyors (FIG), Lisbon, Portugal.
- Salagean, T., Onose, D., Rusu, T., Şuba, E., and Chiorean, S. (2017). Aspects regarding the analysis of horizontal displacements at Cumpana Dam, Arges County. AgroLife Scientific Journal, 6(1):237-242.
- Scaioni, M., Marsella, M., Crosetto, M., Tornatore, V., and Wang, J. (2018). Geodetic and Remote-Sensing Sensors for Dam Deformation Monitoring. Sensors, 18(11):3682, doi:10.3390/s18113682.
- Staroverov, V. and Haikin, D. (2020). Geodesic Monitoring Of Hydrotechnical Structures Using an Automated Observation System. Urban development and spatial planning, 0(74):298-307,

doi:10.32347/2076-815x.2020.74.298-307.

- Szostak-Chrzanowski, A. and Massiéra, M. (2006). Relation between monitoring and design aspects of large earth dams. In Proceedings, 3rd IAG Symposium on Geodesy for Geotechnical and Structural Engineering and 12th FIG Symposium on Deformation Measurements, Baden, Austria. FIG.
- Talich, M. (2016). The Deformation Monitoring of Dams by the Ground-Based InSAR Technique - Case Study of Concrete Hydropower Dam Orlik. International Journal of Advances in Agricultural and Environmental Engineering, 3(1), doi:10.15242/ijaaee.a0416051.
- Taşçi, L. (2008). Dam deformation measurements with GPS. Geodesy and Cartography, 34(4):116-121, doi:10.3846/1392-1541.2008.34.116-121.
- Tretyak, K. and Palianytsia, B. (2022). Research of the environmental temperature influence on the horizontal displacements of the Dnieper hydroelectric station dam (according to GNSS measurements). Reports on Geodesy and Geoinformatics, 113(1):1-10,

doi:10.2478/rgg-2022-0001.

- US Army Corps of Engineers (2018). Structural Deformation Surveying. Engineer Manual EM 1110-2-1009.
- Zaczek-Peplinska, J., Pasik, M., Adamek, A., Adamek, A., Kołakowska, M., and Łapiński, S. (2013). Monitoring Technical Conditions Of Engineering Structures Using The Terrestrial Laser Scanning Technology. Reports on Geodesy and Geoinformatics, 95(1):1-10, doi:10.2478/rgg-2013-0008.
- Zaczek-Peplinska, J., Podawca, K., and Karsznia, K. (2018). Reliability of geodetic control measurements of high dams as a guarantee of safety of the construction and the natural environment. Bulletin of the Polish Academy of Sciences: Technical Sciences, 66(1):87-98, doi:10.24425/119062.
- Šarkanović Bugarinović, M., Govedarica, M., Ristic, A., Bugarinović, Z., and Ruskovski, I. (2023). Analysis and application of terrestrial laser scanning algorithms for dam monitoring. In Proceedings of the International Scientific Conference iNDiS 2023 Planning, Design, Construction and Building Renewal, Vrdnik, Serbia.